Lamellar and Crystalline Layer Thickness of Single Crystals of Narrow Molecular Weight Fractions of Linear Polyethylene

ARTICLE *in* MACROMOLECULES · MAY 2002

Impact Factor: 5.8 · DOI: 10.1021/ma011974u

4 AUTHORS, INCLUDING:

Stéphane Hocquet
Belgian Ceramic Research Centre
18 PUBLICATIONS **80** CITATIONS
SEE PROFILE

Michel Henri Jean Koch
European Molecular Biology Laboratory
413 PUBLICATIONS **16,098** CITATIONS
SEE PROFILE

Lamellar and Crystalline Layer Thickness of Single Crystals of Narrow Molecular Weight Fractions of Linear Polyethylene

S. Hocquet,[†] M. Dosière,*[,†] Y. Tanzawa,[‡] and M. H. J. Koch[§]

Laboratoire de Physicochimie des Polymères, Université de Mons-Hainaut, Place du Parc, 20, B-7000 Mons, Belgium; Department of Systems Engineering, Nagoya Institute of Technology, Gokiso-cho, Showa-ku, Nagoya 466-8555, Japan; and European Molecular Biology Laboratory, Hamburg Outstation, EMBL c/o DESY, Notkestrasse 85, D-22603 Hamburg, Germany

Received November 13, 2001; Revised Manuscript Received March 14, 2002

ABSTRACT: The thermal dependence of the lamellar thickness (L_p) and the thickness of crystalline layers (L_{cryst}) of linear polyethylene single crystals has been revisited. LPE fractions with different average molecular weights were crystallized at the same temperatures to avoid the delicate problem of an arbitrary choice of their equilibrium dissolution temperature to calculate their degree of supercooling. This procedure allows direct check of the thicknesses of the crystalline layers dependence on the degree of supercooling. Indeed, the equilibrium melting and dissolution temperatures depend on the average molecular weight. Mats of linear polyethylene single crystals of various narrow molecular weight fractions were obtained from dilute *p*-xylene solutions. Their lamellar thickness was determined from the SAXS intensity curve. The crystalline layers thickness was calculated from the linear correlation function of the SAXS intensity curves and from the LAM mode frequency of the Raman spectrum. It depends as expected on the crystallization temperature. However, at a given crystallization temperature, both the thicknesses of the lamellae and of the crystalline layers are nearly independent of molecular weight and therefore also of the degree of supercooling estimated from a well-known semiempirical relationship.

Introduction

The main parameters of the kinetic theory of crystallization proposed by Hoffman and Lauritzen[1] (H−L) to explain the morphology and growth of polymers crystals are the degree of supercooling (ΔT), i.e., the difference between the equilibrium melting ($T_m°$) or dissolution ($T_d°$) temperature and the crystallization temperature (T_c), the molecular weight, which would govern the reptation of the macromolecules,[2] and a delay factor generally referred to as the William, Landel, and Ferry (WLF) factor. The conclusions of the kinetic theory can be summarized as follows: crystallization of polymers proceeds with a very small irreversible entropy variation and is governed by a secondary nucleation process. This conclusion implies the existence of several "crystallization regimes" covering the full range of crystallization temperatures for each polymer: a regime of mononucleation (also called "regime I"), a regime of polynucleation (also called "regime II"), and a regime III.[3] The theoretical approach followed by Hoffman et al.[3] presupposes the knowledge of several physical quantities: equilibrium melting temperature $T_m°$, fold surface free enthalpy σ_e, lateral surface free enthalpy σ, kinetic length L_k (i.e., the mean distance between nucleation events), persistence length L_p, initiation rate i (i.e., the frequency of nucleation events per unit length), crystallization temperature T_c, potential barrier U, etc. The precise experimental determination of these parameters is far from evident, as illustrated by the recent controversy about the dependence of melting temperature $T_m°$ on molecular weight.[4] Flory et al.,[5] Broadhurst,[6,7] and Hoffman et al.[8] give a value of 146.5 °C for $T_m°$ of a very high molecular weight linear polyethylene, whereas Atkinson et al.,[9] Wunderlich et al.,[10] and Okada et al.[4] find 141.6 °C.

According to the H−L theory, the initial thickness of a chain-folded lamellar crystal (l) grown from solution is given by $l = \delta l + 2\sigma_e T_d°/\Delta h_m(T_d° - T_c)$, where σ_e is the fold surface enthalpy, $T_d°$ is the equilibrium dissolution temperature, $\Delta T = T_d° - T_c$ is the degree of supercooling corresponding to the crystallization temperature T_c, Δh_m is the melting enthalpy per unit volume, and δl is a nearly constant thickness, the explicit form of which differs in some presentations of the kinetic theory of crystallization.[11−13] It should be stressed that the above relationship is derived on the assumption that the molecular chain length greatly exceeds the lamellar thickness. Plots of lamellar thickness vs reciprocal supercooling have been widely used to estimate δl and the surface enthalpy σ_e assuming a known value for the melting enthalpy. Almost all of these analyses yield a larger δl value than expected from the theory (0.5−1.5 nm).

The lamellar thickness of LPE single crystals can be determined by SAXS and electron microscopy. Also, Raman spectrometry at low shift allows to determine the LAM mode which is related to the length of the chains in the crystalline layers, i.e., the actual length of the trans planar zigzag segments between two successive folds.

In the H−L theory, the values of the lamellar thicknesses are supposed to be known with a precision better than 1 nm and are used in the thermodynamic balance. Experimental studies on the lamellar structure devoted to the thickness of the crystals—one of the main problems concerning the crystallization of semicrystalline polymers—are not sufficiently precise and frequently contradictory.[14−25] Moreover, the consequences of the tilt of the chains with respect to the basal planes of the lamellar crystals and the existence of disordered regions at the two end planes of the lamellae are not

[†] Université de Mons-Hainaut.
[‡] Nagoya Institute of Technology.
[§] European Molecular Biology Laboratory.

10.1021/ma011974u CCC: $22.00
Published on Web 05/21/2002

Table 1. Characteristics and Origin of the LPE Samples[a]

reference	$\langle M_n \rangle$	$\langle M_w \rangle$	p	$T_m°$/°C	$\tau_d°$/°C	$T_d°$/°C	supplier
1482a	11 800	13 600	1.15	142.6	102.7	107.6	NIST[b]
1483	27 900	32 100	1.15	144.8	109.1	111.9	NIST[b]
1475a	18 000	52 300	2.90	143.9	105.0	109.1	NIST[b]
1484a	104 000	119 600	1.15	146.0	113.7	114.8	NIST[b]
	230 300	264 800	1.15	146.2	115.3	115.8	SNPA[c]

[a] $\langle M_n \rangle$ and $\langle M_w \rangle$ are the number- and the weight-average molecular weights, respectively. p is the degree of polydispersity ($\langle M_w \rangle / \langle M_n \rangle$). $T_m°$, $\tau_d°$, and $T_d°$ are the equilibrium melting temperature, the dissolution temperature following Pennings, and the equilibrium dissolution temperature, respectively. [b] National Institute of Standards and Technology (Gaithersburg, USA). [c] Société Nationale des Pétroles d'Aquitaine (now Elf-Atochem, Paris, France).

clearly analyzed, whether for solution or melt crystallization.

In previous works dedicated to the crystallization of LPE from dilute solution, the fold length was usually determined with only one experimental technique. Their conclusions generally do not agree, as summarized hereafter. The fold period of PE single crystals formed at a given temperature determined by SAXS does not vary with molecular length even for a 100-fold change in molecular weight. It does not depend on the concentration of the solution from which the crystals are formed.[14,15] The lamellar thickness of single crystals of fractionated PE crystallized at a given T_c decreases with increasing molecular weight: a difference of 2 nm is observed for samples having viscosity-average molecular weights of 10^4 and 10^5.[17,18] Organ et al.[21] have analyzed single crystals of LPE with a degree of polydispersity of 10 from which the lowest molecular weights have been removed by a preliminary crystallization at 70 °C. The Raman fold lengths of single crystals grown from various solvents do not lie on exactly the same curve in a plot of L_{Ram} vs ΔT. Only the overall trend of dependence of fold length on supercooling is observed. Finally, the lamellar thickness of PE single crystals of low molecular weights (2000−12 000) does not depend on molecular weight at a given T_c. Their dissolution temperature exhibits a definite molecular weight dependence.[25]

The present work deals with the determination of the thicknesses of lamellae (L_p) and the crystalline regions (L_{cryst}) of mats of filtration of LPE single crystals grown from dilute *p*-xylene solution. Several narrow LPE fractions ($\langle M_w \rangle / \langle M_n \rangle \cong 1.15$) covering a wide range of average molecular weights are used to determine whether the thickness of the crystalline layers of the lamellae depends on the degree of supercooling ΔT or on the crystallization temperature T_c. A polydisperse sample is also used to investigate the hypothetical influence of the degree of polydispersity on lamellar as well as crystalline thicknesses. Crystallization from dilute solution was preferred to crystallization from the melt to avoid problems linked with lamellar thickening processes.[26−31] On the contrary, the lamellar thickness of LPE single crystals grown from solution does not vary during crystallization or subsequent storage (even for long periods of time) if the temperature is maintained constant.[32,33] The thicknesses of the (110) and (200) sectors of LPE single crystals will be assumed to be equal although possible differences of the fold length between (110) and (200) sectors have been suggested.[34]

Our approach is based on the fact that the equilibrium dissolution temperature depends on the number-average molecular weight $\langle M_n \rangle$. For LPE single crystals grown from dilute solution in *p*-xylene (0.05 wt %), $T_d°$ is 101.3 and 114.6 °C for $\langle M_n \rangle$ = 10 000 and 100 000, respectively.[35] It results a difference in the ΔT values for these two molecular weights of 13.3 °C, which corresponds to the range of ΔT values usually covered in crystallizations from dilute *p*-xylene solution (75−90 °C). Therefore, single crystals of LPE fractions with different molecular weights crystallized at identical crystallization temperature will be characterized by different degrees of supercooling values: the fraction with the lowest (or highest) molecular weight will have the lowest (or highest) ΔT value. This strategy allows to check experimentally the thermal dependence of the thickness of the crystalline layers of LPE single crystals without having to deal with the true value of the equilibrium dissolution temperature of LPE.

Experimental Section

Materials. The molecular characteristics and the origin of the LPE samples are given in Table 1.

Crystallization from Dilute Solution in *p*-Xylene. LPE fractions at 0.05% concentration (w/w) were dissolved in boiling *p*-xylene under nitrogen. After crystallization at a given temperature using the self-seeding technique,[44] the solution was slowly filtered using a Buchner funnel fitted with a PTFE filter (porosity 3) maintained at the crystallization temperature. The mats of LPE single crystals were washed with acetone and dried under vacuum at 50 °C for 24 h to remove the last traces of solvent. This procedure yields well-oriented mats of filtration of single crystals.

Techniques. (a) X-ray Diffraction (SAXS and WAXD). Ni-filtered Cu Kα radiation from a point focus rotating anode (Rigaku RU200) was used to record the two-dimensional WAXD and SAXS patterns on image plates with a modified Kiessig camera (pinhole collimation). Square image plates with an area of about 140 cm^2 were scanned with 50 μm resolution on a Fuji X BAS-3000 imaging analyzer yielding 12 bits intensity data. The range of scattering vector is $1/(1.5\text{ nm}) < s < 1/(0.45\text{ nm})$ ($s = 2 \sin\theta/\lambda$, where 2θ is the scattering angle and λ the wavelength of the incident X-ray beam (0.154 18 nm)). The following operations were performed on the WAXD data using the "X-ray" software:[37] (i) automatic search of the center of the X-ray pattern, (ii) background subtraction, (iii) Lorentz and polarization corrections, (iv) angular integration of the pattern to obtain intensity profiles, (v) analysis of the intensity profiles: peak fitting and integration, and (vi) determination of the parameters of the unit cell. The profiles of the (200) and (020) diffraction were obtained by circular integration.

The SAXS curves were also recorded for 180 s with a linear position-sensitive detector on the D1/2 beam line of the EMBL in HASYLAB on the storage ring DORIS III of the Deutsches Elektronen Synchrotron (DESY) at Hamburg.[38,39] The wavelength of the incident X-ray beam was 0.15 nm. The SAXS intensities were recorded in the range $1/(70\text{ nm}) < s < 1/(3\text{ nm})$. The calibration of the detector channels in terms of scattering vector was made by linear regression over the positions of numerous orders of the long spacing of dry collagen (L_p = 65 nm). The thickness of the crystalline (L_{cryst}) and the amorphous (L_{am}) layers, the long period (L_p), and the linear degree of crystallinity (v_c^{lin}) were obtained from the linear correlation function according to standard procedures.[40]

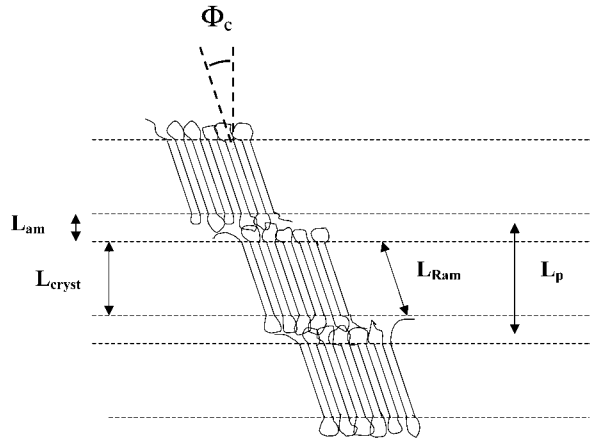

Figure 1. Schematic drawing of a lamellar stack with its characteristic parameters: lamellar thickness or long spacing (L_p), thickness of amorphous (L_{am}) and crystalline (L_{cryst}) regions, mean chain length in the crystal core ($L_c = L_{Ram}$).

(b) Electron Diffraction. A drop of the LPE single crystals suspension was deposited on a glass slide, and the solvent was let to evaporate. The glass slide was coated with a thin carbon film. Suitable areas were removed from the glass slide by flotation with poly(acrylic acid) and mounted on electron microscopy grids. In the electron microscope (Philips CM12), each isolated single crystal was rotated around its crystallographic *a*-axis until a two-dimensional electron diffraction pattern corresponding to the *a***b** reciprocal plane was obtained. The rotation angle read on the tilting stage is a direct measure of the tilt of the chains, Φ_c.

(c) Raman Spectrometry. Raman spectra at low shifts (5−100 cm^{-1}) of filtration mats of LPE single crystals were recorded with a XY800 Raman spectrometer. A triple monochromator allows to record spectra at very low wavenumbers near the Rayleigh line. An argon laser delivered an incident radiation power on the filtration mats of 10−20 mW at 514 nm. The Raman spectra were recorded in 10 s time frames using a 512 channels array detector cooled with liquid nitrogen. The wavenumber of the LAM mode is inversely proportional to the length of the chains in zigzag conformation.[41]

(d) Differential Scanning Calorimetry. DSC was used as a convenient technique to check the drying of the mats of filtration. A heat flux differential scanning calorimeter (TA Instruments, model 2920) working under helium atmosphere with a scanning rate of 10 °C/min was used. Temperature and heat flow were calibrated with benzoic acid, indium, and zinc standards. A baseline obtained with two empty pans was subtracted from the melting curves.

Results

Lamellar Morphology. The schematic representation of a mat of filtration of well-sedimented single crystals (Figure 1) helps to define the lamellar thickness equated with the long spacing (L_p), the thicknesses of the crystalline (L_{cryst}) and amorphous (L_{am}) layers, and finally the length of a stem in the crystalline core along the chain axis (L_c) identified to the spacing obtained from Raman spectrometry at low shifts (L_{Ram}). Typical SAXS and WAXD patterns obtained from a filtration mat of LPE single crystals ($\langle M_w \rangle = 32\,100$) crystallized from a dilute solution in *p*-xylene at 85 °C are shown in parts a and b of Figure 2, respectively. The SAXS intensity is mainly distributed along arcs spanning a range of ±30° with respect to the normal to the plane of the mat (Figure 2a). The intensity curve is obtained by azimuthal integration of the two-dimensional SAXS pattern. The SAXS intensity curve has been also recorded with a linear position-sensitive detector (Figure 2c). The values of the long spacing L_p and the subsequent orders of the LPE samples ($\langle M_w \rangle = 32\,100$) are given in Table 2 for the different crystallization temperatures T_c. In some cases, SAXS data were recorded on a second mat of filtration prepared under identical conditions to check the accuracy of these SAXS measurements. The lamellar thicknesses reported in Table 2 and Figure 3 are accurate within ±0.15 nm. An experimental error of ±0.25 nm was found only once for all the long spacing data reported in this work.

Tilt of the Chain Axes in the Crystalline Layers of Lamellar Crystals. The tilt of the chain axes (ϕ_c) can be derived from $\cos^2 \phi_a + \cos^2 \phi_b + \cos^2 \phi_c = 1$, where the angles ϕ_a and ϕ_b are obtained from the intensity profiles of the (200) and (020) reflections, respectively. The profiles of the intensity of the (200) and (020) reflections of the WAXD pattern of a mat of LPE single crystals, obtained with the incident X-ray beam oriented along the plane of the mat, are given in Figure 4. The values of ϕ_c for the different LPE fractions are given as a function of the crystallization temperatures in Figure 5.

Chain Length in the Crystal Core of the Lamellar Crystals. First, the constant *K* linking the Raman shift to the crystalline stem length L_{Ram} was experimentally reexamined using the LAM spectra of several ultralong *n*-paraffins with known morphology.[42] The number of folds per chain was determined from the SAXS patterns: the thickness of the crystalline layers was identified with the long spacing assuming a sharp fold conformation.[43] Experimental results are given in Table 3 and in Figure 6. The best least-squares fit yields 295 GPa for the elastic modulus, very close to 290 GPa proposed by Strobl et al.[44] but significantly different from other previously reported values.[41,45−48] The thickness of the crystalline layers of single crystals of LPE fractions have been also estimated from Raman spectroscopy at low shift. Indeed, the most probable length of the crystalline stem along the chain axis L_{Ram} can be measured from the LAM mode using the well-known relationship $L_{Ram} = K/\Delta\nu$, where $\Delta\nu$ is the frequency of the longitudinal acoustic mode (LAM) vibrations given in cm^{-1}. *K* is a constant equal to $m(E/\rho)^{1/2}/2c$, where *m* and *c* are the order of the LAM mode and the velocity of light, respectively.[41] The frequency distribution was converted to the fold length distribution by multiplying the Raman intensity at frequency ν by a factor $K\nu^2$ after subtraction of a suitable background. The corrected L_{Ram} values, i.e., the chain length L_c along the chain axis in the crystalline layers, are plotted against T_c for the different LPE fractions in Figure 7. L_{Ram} increases with T_c but is nearly independent of molecular weight for each crystallization temperature (±0.5 nm at most).

Discussion

Thicknesses of the Lamellae and of the Crystalline Layers. The occurrence of several orders of the long spacing in the SAXS patterns (Figure 2a,c and Table 2) indicates that the mats of filtration are made of stacks of lamellae with a sharp distribution of lamellar thicknesses at all investigated crystallization temperatures. The lamellar thickness given by the long period L_p of different LPE single crystals continuously increases with the crystallization temperature (Figure 3). The difference between the smallest and the largest L_p values for the different fractions at a given crystallization temperature is about 0.7 nm for $77.2 < T_c <$

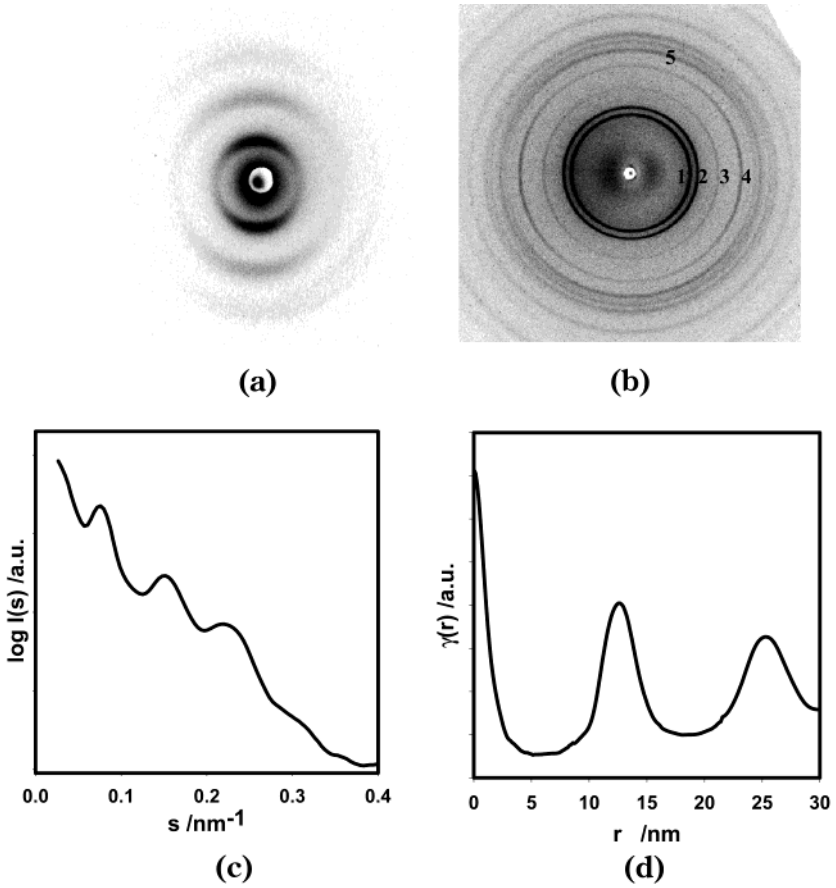

Figure 2. Two-dimensional SAXS (a) and WAXD (b) patterns of a filtration mat of LPE single crystals obtained with the X-ray beam in the plane of the mat; the normal to the plane of the mat is vertical. Wide-angle X-ray diffractions are labeled as 1, (110); 2, (200); 3, (210); 4, (020); (c) corrected SAXS pattern recorded with a linear position-sensitive detector; and (d) linear correlation function $\gamma(r)$ corresponding to the SAXS curve displayed in (c).

Table 2. Lamellar Thickness (L_p), Thicknesses of Crystalline (L_{cryst}) and Interface (L_{am}) Regions, Linear Degree of Crystallinity (ν_c^{lin}), Tilt of the Chains (Φ_c), Raman LAM Mode ($\Delta\nu_{Ram}$), Corrected Raman LAM Mode ($\Delta\nu_{cor}$), Length of the Chains in Crystalline Regions (L_{Ram}^{cor}), and Thickness of Crystalline Regions from Raman Data (L^*_{cryst})

T_c/ °C	$L_p(1)$/ nm	$L_p(2)$/ nm	$L_p(3)$/ nm	L_p(cfu)/ nm	L_{cryst}/ nm	L_{am}/ nm	ν_c^{lin}	Φ_c/ deg	$\Delta\nu_{Ram}$/ cm^{-1}	$\Delta\nu_{cor}$/ cm^{-1}	L_{Ram}^{cor}/ nm	L^*_{cryst}/ nm
77.2	11.42	5.71	3.78	11.10	8.99	2.11	0.81	0	27.48	27.48	10.35	10.35
	11.17	5.63	3.75	10.90	8.83	2.07	0.81	19	26.22	27.48	10.35	9.79
79.8	11.95	5.93		11.80	7.67	4.13	0.65	0	25.64	26.32	10.81	10.81
82.3	12.54	6.24	4.14	12.30	9.59	2.71	0.78	22	24.44	24.44	11.64	10.79
	12.54	6.24	4.12	12.40	8.18	4.21	0.66	19	24.44	25.07	11.34	10.72
84.9	12.96	6.45		12.70	10.16	2.54	0.81	24	22.55	23.18	12.27	11.21
	13.07	6.45		13.00	10.66	2.34	0.82	26				
87.3	14.55	7.14	4.65	13.90	11.95	1.95	0.86	13	20.66	22.55	12.61	12.29
89.9	14.97	7.49	4.96	14.70	12.40	2.30	0.84	29	20.42	20.42	13.93	12.18

87.3 °C but increases to 0.87 and 1.5 nm for $T_c = 87.3$ and 89.9 °C, respectively. The thickness of single crystals of LPE fractions is almost independent of $\langle M_n \rangle$ at any given crystallization temperature.

The linear correlation function $\gamma(r)$ calculated from the SAXS pattern (Figure 2d) also yields both the crystalline and amorphous layers thicknesses.[40] As the weight degree of crystallinity of the LPE filtration mats estimated by DSC is around 0.8, the crystalline layer thickness (L_{cryst}) can be unambiguously attributed to the largest of the two values, i.e., L_2. In Figure 8, L_{cryst} for mats of different $\langle M_n \rangle$ is plotted against crystallization temperature. There is a 100% increase of L_{cryst} with both T_c and $\langle M_n \rangle$.

The fold length distributions obtained by multiplying the Raman intensity at frequency ν by a factor $K\nu^2$ yields the most probable chain length and its dispersion (half-width at half-height of the curve) for each sample. The most probable chain lengths are given vs crystallization temperature for the various fractions (Figure 7). Since values of half-width at half-height of the distribution are below 1 nm, the distribution of chain lengths is also narrow for all fractions and all crystallization temperatures. This result also stems from the identity between the uncorrected and corrected values of the LAM frequency (Table 2). The thickness of the crystalline layers L_{cryst} from the LAM data and the length of the chains in the crystal core L_c must be corrected for the tilt of the chains: $L_{cryst} = L_c \cos \phi_c \cong L_{Ram} \cos \phi_c$. Indeed, during filtration of the suspension of LPE single crystals and the subsequent drying, single crystals are flattened and the chains can tilt by a angle Φ_c with respect to the normal to the basal planes of the lamellae. The Φ_c values range between 19° and 45° for

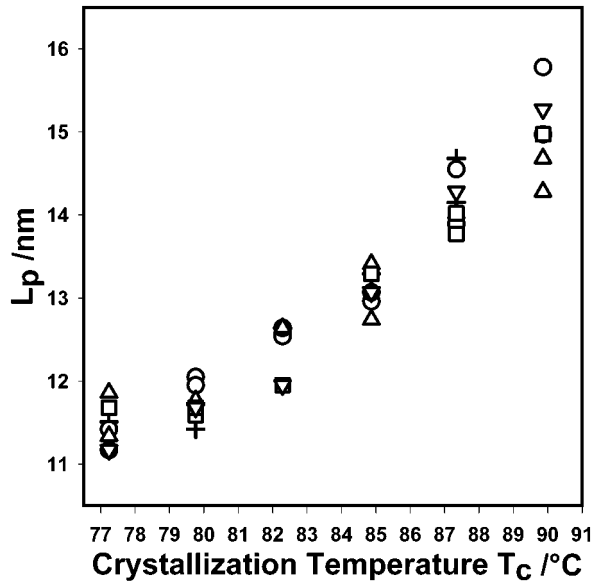

Figure 3. Long period (L_p) or lamellar thickness of LPE single crystals obtained from dilute solution in *p*-xylene vs crystallization temperature T_c for $\langle M_w \rangle$ = 13 600 (+), 32 100 (○), 52 300 (△), 119 600 (□), and 264 800 (▽).

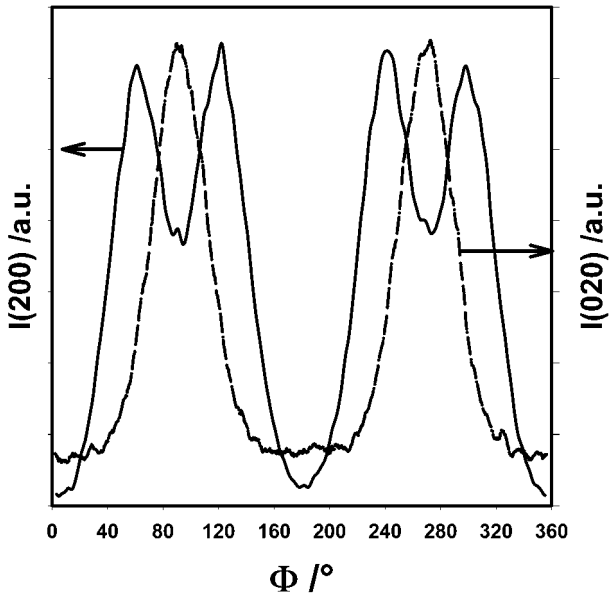

Figure 4. Profiles of the (200) and (020) WAXD reflections of an oriented filtration mat of LPE single crystals.

(101) up to (301) end planes.[49,50] The tilt correction is not frequently made. The reason can be found perhaps in the following numerical example illustrating the opposing effects of corrections which sometimes can compensate each other. For a degree of crystallinity of 80−90%, a typical value for LPE single crystals, the thickness of the crystal core (L_{cryst}) is between 23 and 11% lower than the long spacing L_p determined by SAXS. However, because of the tilt of the chains with respect to the basal planes of the lamellae, the length of the chains L_c in the crystalline layers will be 6, 22, or 41% larger than the thickness of the crystalline layers L_{cryst} for (101), (201), or (301) fold surfaces. The tilt angle of the chains for LPE fractions tends to increase with increasing T_c (Figure 5). There is generally a good agreement between the mean ϕ_c values obtained by X-ray diffraction on mats of filtration and those determined by electron diffraction on individual single crys-

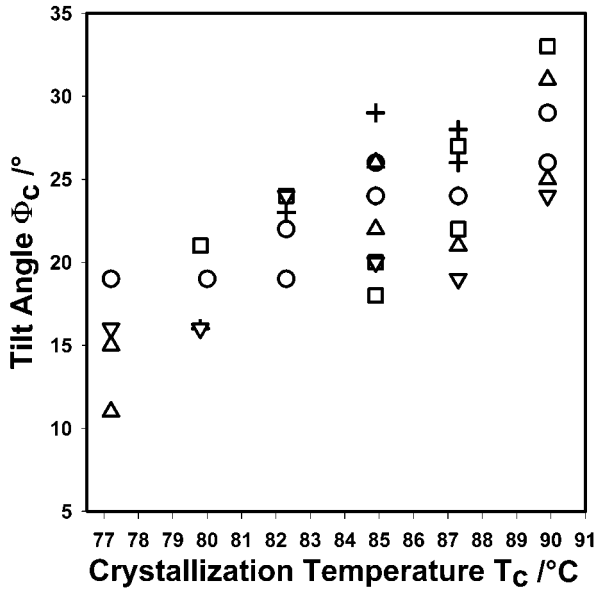

Figure 5. Tilt angle (Φ_c) of the chains in the crystalline layers of an oriented filtration mat of LPE single crystals. $\langle M_w \rangle$ = 13 600 (+), 32 100 (○), 52 300 (△), 119 600 (□), and 264 800 (▽).

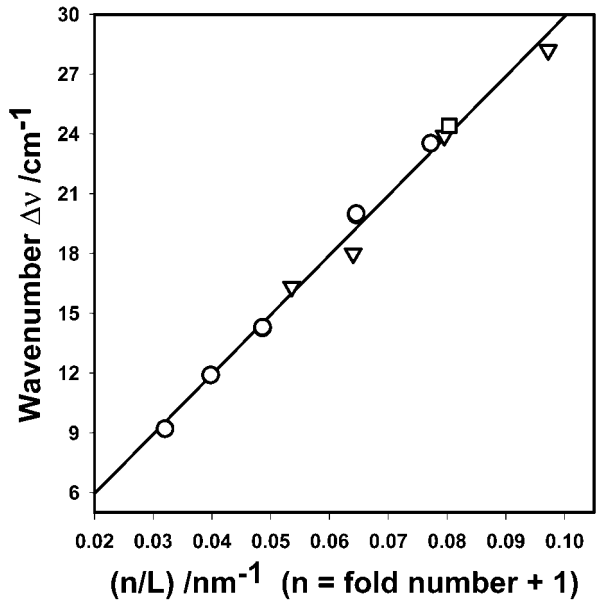

Figure 6. Raman shift of ultralong paraffins vs length of the chains in the crystalline layers: ○, extended chains crystals; ▽, 1-integral folded chains crystals; □, 2-integral folded chains crystals.

Table 3. LAM Wavenumber and Number of Folds for Various Ultralong Paraffins

no. of C atoms	no. of folds	$\Delta\nu$/cm^{-1}	no. of C atoms	no. of folds	$\Delta\nu$/cm^{-1}
102	0	23.5_3	246	0	9.2_0
122	0	19.9_3	162	1	28.2_0
122	0	20.0_0	198	1	23.9_0
162	0	14.2_6	246	1	18.0_0
162	0	14.3_0	294	1	16.3_3
198	0	11.9_0	294	2	24.4_0

tals. We assume that the chain axes have a quasi-constant orientation in the (110) and (200) sectors of the lozenge-shaped LPE single crystals grown in a good solvent (e.g., *p*-xylene), in contrast to the situation observed in single crystals formed in poor solvents.[51] The L_{cryst} values for LPE single crystals of different

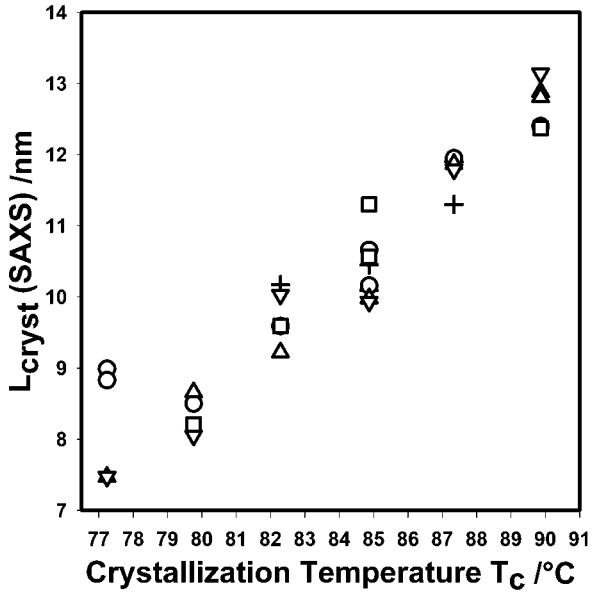

Figure 7. Thickness of crystalline layers (L_{cryst}) of LPE single crystals calculated from the correlation function of SAXS data vs crystallization temperature T_c for different $\langle M_w \rangle$ = 13 600 (+), 32 100 (○), 52 300 (△), 119 600 (□), and 264 800 (▽).

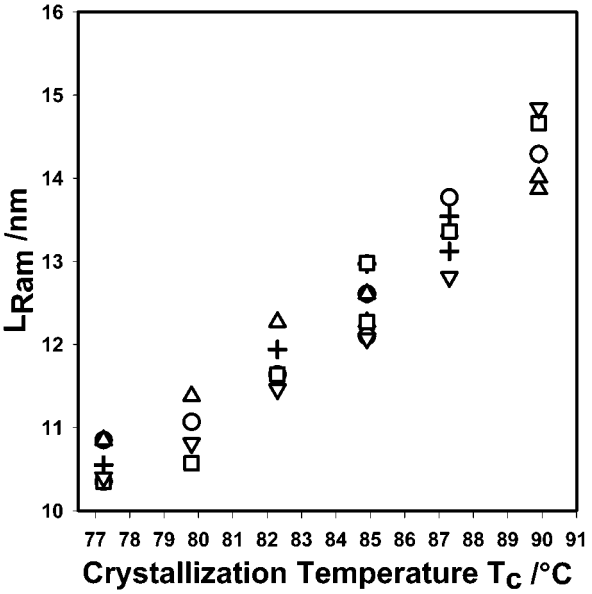

Figure 8. Chain length L_{Ram} in LPE single crystals calculated from the LAM Raman shift vs crystallization temperature T_c for $\langle M_w \rangle$ = 13 600 (+), 32 100 (○), 52 300 (△), 119 600 (□), and 264 800 (▽).

molecular weights obtained from LAM mode data are plotted vs T_c (Figure 9). L_{cryst} values estimated from LAM mode and SAXS data are similar. Some small differences for thicknesses estimated from Raman spectroscopy could result from some scatter in the estimated ϕ_c values and some small inaccuracy in the calibration of the LAM data from SAXS measurements.[52] The thicknesses of the crystalline layers of single crystals of LPE fractions with different molecular weights are approximately equal for each T_c and do not display the expected dependence on the degree of supercooling. This is the main conclusion of the present work based on experimental data and a fully accepted dependence of the equilibrium dissolution temperature on the molecular weight as explained in the next section.

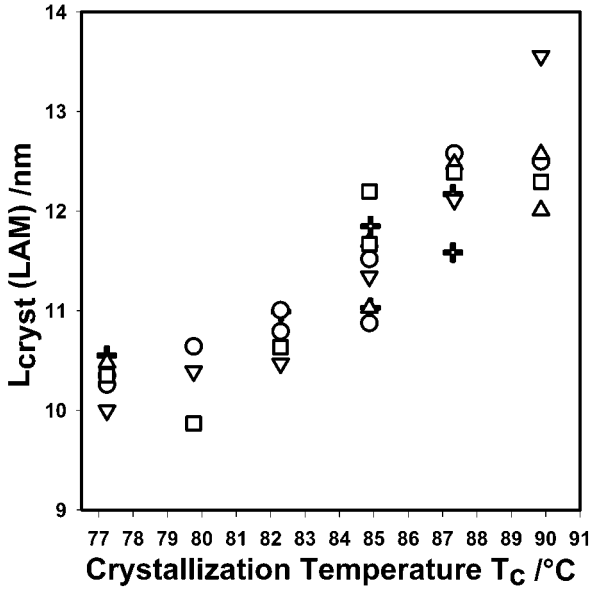

Figure 9. Thickness of the crystalline layers L_{cryst} calculated from the LAM measurements and the tilt of the chains (Φ_c) vs crystallization temperature T_c for different $\langle M_w \rangle$ = 13 600 (+), 32 100 (○), 52 300 (△), 119 600 (□), and 264 800 (▽).

Degree of Supercooling of the Various LPE Fractions. Several experimental methods have been used to determine the equilibrium dissolution temperature $T_d°$: (a) The dissolution temperature of PE crystals of known lamellar thickness is extrapolated to infinite thickness.[18,24,53−55] Such a method has been reported not to be sufficiently sensitive to detect the dependence of $T_d°$ on $\langle M_n \rangle$. (b) The dissolution temperature of extended chain crystals has been identified to $T_d°$. Such an approach has been only applied to a few LPE fractions covering a restricted range of molecular weights.[4] (c) A following semiempirical relationship[56] has been suggested to estimate the equilibrium dissolution temperature $T_d°$ of LPE in *p*-xylene: $T_d° = (T_m° + \tau_d° - 29)/2$, where $T_d°$, $T_m°$, and $\tau_d°$ are the equilibrium dissolution temperature, the equilibrium melting temperature according to Broadhurst[6,7] and Hoffman,[8] and the dissolution temperature following Pennings,[57] respectively. $T_m°$, $\tau_d°$, and $T_d°$ in *p*-xylene for the various LPE samples used in this work are given in Table 1. In Table 1 of ref 35 are given $T_d°$ values for LPE samples with molecular weights and concentrations in *p*-xylene solution ranging between 10^4 and 10^6 and 10^{-3} and 10 g LPE/100 mL solvent, respectively. These estimated values of the equilibrium dissolution temperature $T_d°$ in *p*-xylene for a concentration of 0.05 wt % are plotted against the number-average molecular weight of LPE samples in Figure 10. From the range of $T_d°$ covered in this work by the various sharp LPE fractions, the degree of supercooling for the samples with lowest and highest $\langle M_n \rangle$ differs by 13.1 °C at any T_c. The thickness of the crystalline layers of LPE single crystals is plotted against the reciprocal value of the degree of supercooling ΔT for the various LPE fractions in Figure 11a,b. In Figure 11a, a given symbol corresponds to a given T_c and includes therefore data relative to all LPE fractions. The thickness of the crystalline layers of the different LPE fractions at each T_c remains approximately constant even though the ΔT values for the fractions with extreme molecular weights differ by up to 13 °C. The lines drawn through data in Figure 11a are mean on all thicknesses of crystalline layers obtained at each T_c

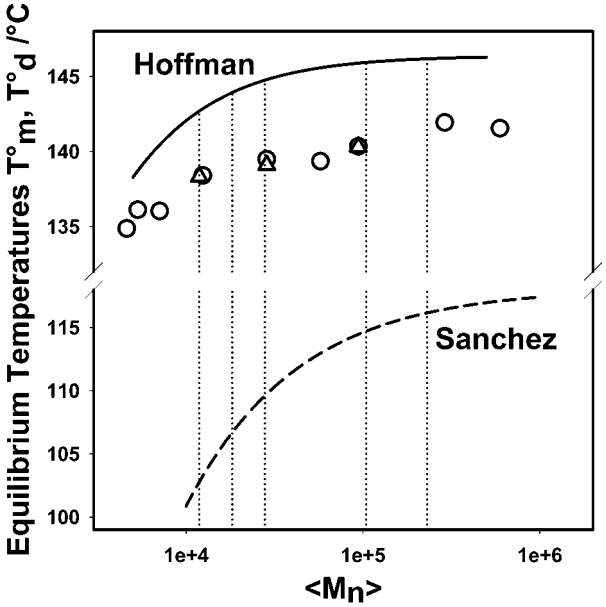

Figure 10. Equilibrium melting temperature $T_m°$ for polyethylene vs the number-average molecular weight ($\langle M_n \rangle$). Experimental values obtained from extended chain crystals: △, Hikosaka et al.; ○, Wunderlich. (—) Extrapolated values for $T_m°$ proposed by Hoffman et al. (- - -) Equilibrium dissolution temperatures $T_d°$ for LPE in *p*-xylene solution (0.05 wt %) vs $\langle M_n \rangle$ calculated from the semiempirical relation proposed by Sanchez et al.[56]

for the various fractions. The best least-squares fitted lines have been also represented in dashed lines in Figure 11a. These observations demonstrate that there is no expected dependence of the thickness of the crystalline layers on $(\Delta T)^{-1}$ at any of the crystallization temperatures for any LPE fraction even at the highest crystallization temperatures where the slope ($\Delta L_{cryst}/\Delta T_c$) takes its largest value. Such data are quite opposite to all conclusions reached in a large number of previous works where sometimes some authors report that "only a trend is observed in a plot of L_c versus $(\Delta T)^{-1}$".[21] We have therefore plotted our results in the "conventional" way (Figure 11b) where the thicknesses of the crystalline layers of each fraction crystallized at various T_c are represented by the same symbol. Each line in Figure 11b represents the best fit based on the relationship $L_{cryst} \propto (\Delta T)^{-1}$ for a given fraction. In Figure 11a,b, each set of data are spread on quasi-identical degrees of supercooling: 12.6 °C resulting from the difference between the highest and the lowest crystallization temperatures (89.9−77.2 °C) in Figure 11b and 13.1 °C in Figure 11a resulting from the difference between the highest and lowest equilibrium dissolution temperatures for the lowest and the highest molecular weight fraction. Such a result is particularly intriguing since both treatments use the same set of experimental data (thicknesses of crystalline layers obtained from SAXS and LAM) and calculated equilibrium dissolution temperatures. This result suggests that depending on how one plots data, what defines L_{cryst} is either T_c or ΔT.

Is there a way to explain such a conflicting representation? The presence of at least 3 orders of the long spacing of LPE single crystals is a strong argument in favor of the quality and precision of the SAXS data used to calculate the lamellar and the crystalline layers thicknesses. The mathematical procedure that yields the linear correlation function from the SAXS pattern is a well-established procedure. Crystallization temperatures have been measured within ±0.05 °C and were recorded during all crystallization experiments. The relationship between wavenumber and chain length has been verified using ultralong paraffins, the best "standards" presently available for such a calibration. The experimental data and their treatment cannot be the cause for the different behaviors.

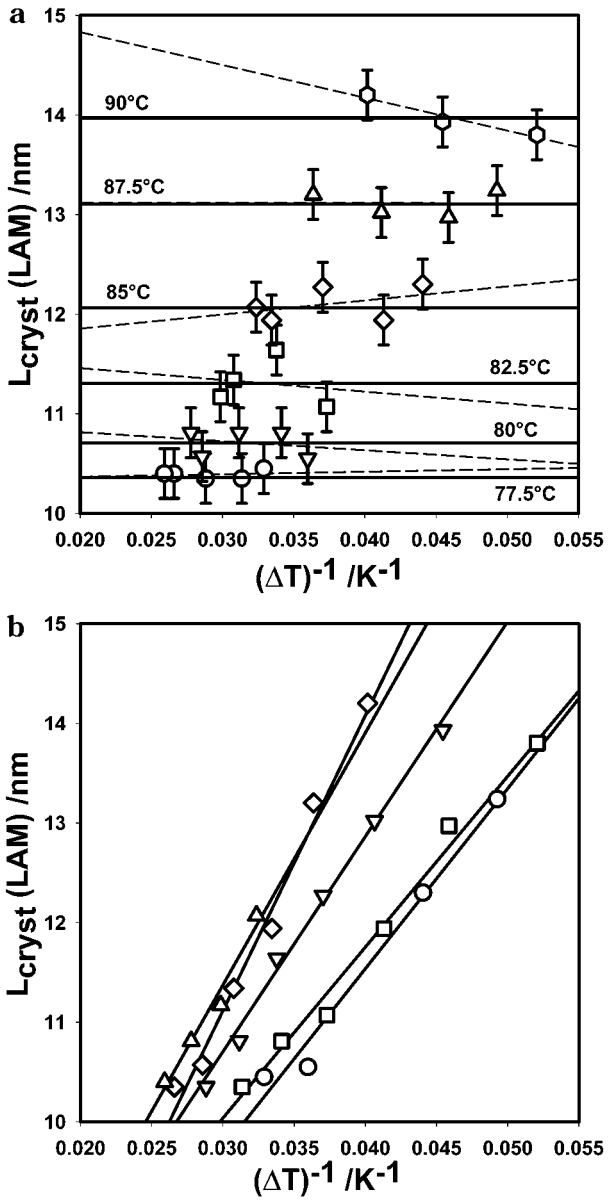

Figure 11. Crystal thickness L_{cryst} of LPE single crystals obtained from dilute solution in *p*-xylene vs the reciprocal value of the degree of supercooling ΔT: (a) each symbol corresponds to a given crystallization temperature and therefore represents samples with different molecular weights (○, T_c = 77.2 °C; ▽, T_c = 79.8 °C; □, T_c = 82.3 °C; ◇, T_c = 84.9 °C; △, T_c = 87.3 °C; ⬡, T_c = 79.9 °C); the crystallization temperatures have been printed in the figure. (b) Each symbol corresponds to different crystallization temperatures for a given LPE fraction ("conventional" treatment) (○, $\langle M_w \rangle$ = 13 600; ▽, $\langle M_w \rangle$ = 32 100; □, $\langle M_w \rangle$ = 52 300; ◇, $\langle M_w \rangle$ = 119 600; △, $\langle M_w \rangle$ = 264 800). Crystal thickness data used in these figures have been obtained from LAM measurements. Similar figures can be drawn from SAXS data. In (a), the dashed lines are the best least-squares fitted lines, and the horizontal lines have been drawn from the mean of all data relative at a given crystallization temperature.

Figures 8 and 9 indicate that the crystalline layer thickness of narrow molecular weight fractions of LPE

crystallized in the range of 77.2−89.9 °C is constant within ±0.5 nm at constant crystallization temperature. This means that the thickness of the crystalline layers barely depends on the average molecular weight. It also suggests that the dependence of the equilibrium dissolution temperature on the number-average molecular weight is overestimated. Indeed, the values of $T_d°$ calculated from the semiempirical relation continuously increase with respect to $\langle M_n \rangle$, the asymptotic $T_d°$ value being only reached for $\langle M_n \rangle$ values larger than 500 000 (Figure 10).

In this context, it seems useful to compare and to contrast calculated melting and dissolution equilibrium temperatures. Broadhurst,[6,7] Hoffman et al.[8] on one side, and Wunderlich[58] on the other side have proposed two methods to determine the $T_m°$ of LPE. In the first method, $T_m°$ is extrapolated from the observed molecular weight dependence of the melting of *n*-alkanes, theoretically taking into account the effect of chain ends on the melting temperature. In the second, $T_m°$ is estimated by extrapolation of the measured melting temperature of extended chain crystals plotted against the reciprocal value of their thickness (Gibbs−Thomson relation). Extended chain LPE crystals that are a few microns thick melt 0.3 °C below the equilibrium melting temperature $T_m°$. For LPE extrapolated at infinite molecular weight, the two methods give $T_m°$ values of 146.5 and 141.6 °C, respectively (Figure 10). As these two values differ by 5 °C, this amounts to nearly 20% difference for the estimated ΔT values. There is no agreement as to which method gives the correct value for the equilibrium melting temperature $T_m°$ of LPE, the most investigated semicrystalline polymer. Data of Okada et al.[4] are also included in Figure 10. The asymptotic behavior of the two sets is different: the data obtained from the extrapolation method (Broadhurst, Hoffman et al.) display a small variation (0.5 °C) of $T_m°$ for $\langle M_n \rangle$ ranging between 50 000 and 10^6. A larger variation of $T_m°$ (1.8 °C) is observed for melting temperatures obtained on extended chain crystals. However, the situations are quite different for dissolution and melting. For LPE samples with number-average molecular weights of 11 800 and 230 000, the difference in the equilibrium dissolution temperature is 13.1 °C, although these differences should be only 4.1 and 3 °C from the two estimates of the equilibrium melting temperatures (Figure 10). This means that the dependence of temperature $T_d°$ on $\langle M_n \rangle$ calculated from the semiempirical relation proposed by Sanchez et al.[56] is at least 3−4 times larger than that of the melting temperature $T_m°$: $[\Delta T_d°/\Delta\langle M_n \rangle] \geq 3[\Delta T_m°/\Delta\langle M_n \rangle]$.

Let us examine why the values of the equilibrium dissolution temperature of LPE fractions in *p*-xylene obtained from the semiempirical relation proposed by Sanchez et al. seem to be inaccurate. The relationship is based on chemical thermodynamics considerations and applies therefore to homogeneous solution or phase. It should be realized that crystallization from solution is a nonsteady regime with variation of concentration, molecular weight, molecular weight distribution, etc., both in space and in time. The concentration near the growth front upon attachment of the depositing molecule is higher than the overall concentration. Hobbs et al.[59] have shown that the concentration has little impact on the dissolution temperature for chains as short as $C_{198}H_{398}$. According to these authors, the theoretical calculation of the chemical potential of the solvent and the crystal at high dissolution is flawed. Depletion of the overall concentration and a molecular weight fractionation in the course of crystallization are most likely and have been invoked to explain the slowdown of the linear growth rate G_{110} of PE single crystals.[60−63] Because of fractionation, when the crystallization is stopped before complete exhaustion of LPE in the solution, the molecular weight of the crystallized LPE is larger than that of the LPE remaining in solution.[63] For oligomers of ethylene, it has been shown that dissolution temperatures of LPE fractions calculated from the semiempirical relation of Sanchez et al. were inaccurate.[64]

The inaccuracy of the calculated values of the degree of supercooling is certainly the main reason for the conflicting representation of our results summarized in Figures 11. The next step to solve this conflicting situation requires a determination as accurate as possible of the equilibrium dissolution temperature of the LPE fractions. This work is in progress along two directions: (a) determination of the dissolution temperature of extended chain crystals of the various fractions; (b) extrapolation of the dissolution temperature of LPE single crystals of known thickness obtained with the isochronous decoration technique[65] to infinite thickness.

Conclusions

The dependence of the lamellar and crystalline layers thicknesses of LPE single crystals on the degree of supercooling has been reinvestigated by applying a strategy in which LPE fractions with different $\langle M_n \rangle$ are crystallized at identical T_c. For narrow LPE fractions with molecular weights ranging between 11 800 and 230 300, the degree of supercooling differs by 13.1 °C at each T_c, as estimated from the semiempirical relation proposed par Sanchez et al.[56] The crystalline layers thickness has been determined from SAXS linear correlation functions and the Raman LAM mode. Virtually no dependence of the crystalline layer thickness on the degree of supercooling was observed for T_c ranging between 77.2 and 89.9 °C. However, a conventional analysis of the crystalline thickness of an LPE sample crystallized at various temperatures leads to the conclusion that L_{cryst} is inversely proportional to ΔT. Such quite opposite conclusions regarding the thermal dependence of the thickness of the crystalline layers of LPE single crystals using the same set of corrected experimental data recorded with two independent experimental techniques (SAXS and Raman spectrometry) are particularly intriguing. Our analysis of these discrepancies leads us to question the validity of the equilibrium dissolution temperatures obtained with the semiempirical relation proposed by Sanchez et al. Indeed, these values appear to be overestimated for the various LPE fractions used in the present work. Experimental determination of the equilibrium dissolution temperature of LPE fractions by two different procedures is in progress.

Acknowledgment. This work was supported by the Belgian National Fund for Scientific Research (F.N.R.S.) and the European Union through the HCMP Access to Large Installation Project, Contract HPRI-CT-1993-00017 to the EMBL. S. Hocquet acknowledges the Belgian National Fund for Scientific Research of Belgium for a PhD grant. The authors thank Dr. B. Lotz for fruitful discussions and discerning comments.

References and Notes

(1) Lauritzen, J. I., Jr.; Hoffman, J. D. *J. Res. Natl. Bur. Stand. (U.S.)* **1960**, *A64*, 73.
(2) Marand, H.; Mansfield, M. L. *Macromolecules* **1998**, *31*, 5563.
(3) Hoffman, J. D.; Miller, A. *Polymer* **1997**, *38*, 3151.
(4) Okada, M.; Nishi, M.; Takahashi, M.; Matsuda, H.; Toda, A.; Hikosaka, M. *Polymer* **1998**, *39*, 4535.
(5) Flory, P. J.; Vrij, A. *J. Am. Chem. Soc.* **1963**, *85*, 3548.
(6) Broadhurst, M. G. *J. Chem. Phys.* **1962**, *36*, 2578.
(7) Broadhurst, M. G. *J. Res. Natl. Bur. Stand. (U.S.)* **1966**, *70A*, 481.
(8) Hoffman, J. D.; Frolen, L. J.; Ross, G. S.; Lauritzen, J. I. *J. Res. Natl. Bur. Stand. (U.S.)* **1975**, *79A*, 671.
(9) Atkinson, C. M. L.; Richardson, M. J. *Trans. Faraday Soc.* **1969**, *65*, 1749.
(10) Wunderlich, B.; Czornyj, G. *Macromolecules* **1977**, *10*, 960.
(11) Lauritzen, J. I., Jr.; Hoffman, J. D. *J. Res. Natl. Bur. Stand. (U.S.)* **1960**, *A64*, 73.
(12) Frank, F. C.; Tosi, M. *Proc. R. Soc. London, Ser. A* **1961**, *263*, 323.
(13) Gornick, F.; Hoffman, J. D. *Ind. Eng. Chem.* **1966**, *58*, 41.
(14) Keller, A.; O'Connor, A. *Polymer* **1960**, *1*, 163.
(15) Bassett, D. C.; Keller, A. *Philos. Mag.* **1961**, *6*, 344.
(16) Kawai, T.; Keller, A. *Philos. Mag.* **1965**, *11*, 1165.
(17) Kawai, T.; Hama, T.; Ehara, K. *Makromol. Chem.* **1968**, *113*, 282.
(18) Hamada, F.; Korenaga, T.; Nakajima, A. *Polym. J.* **1976**, *8*, 341.
(19) Organ, S.; Keller, A. *J. Mater. Sci.* **1985**, *20*, 1571.
(20) Organ, S.; Keller, A. *J. Mater. Sci.* **1985**, *20*, 1586.
(21) Organ, S.; Keller, A. *J. Mater. Sci.* **1985**, *20*, 1602.
(22) Miller, R. L. *Kolloid Z. Z. Polym.* **1968**, *225*, 62.
(23) Nakajima, A.; Hamada, F.; Hayashi, S.; Sumida, T. *Kolloid Z. Z. Polym.* **1967**, *222*, 10.
(24) Nakajima, A.; Hayashi, S.; Korenaga, T.; Sumida, T. *Kolloid Z. Z. Polym.* **1967**, *222*, 124.
(25) Leung, W. H.; Manley, R. St.; Panaras, A. R. *Macromolecules* **1985**, *18*, 746.
(26) Hoffman, J. D.; Weeks, J. J. *J. Chem. Phys.* **1965**, *42*, 4301.
(27) Kovacs, A. J.; Gonthier, A.; Straupe, C. *J. Polym. Sci., Part C* **1975**, *50*, 283.
(28) Dlugosz, J.; Fraser, G. V.; Grubb, D.; Keller, A. Odell, J. A.; Goggin, P. L. *Polymer* **1976**, *17*, 471.
(29) Barham, P. J.; Keller, A. *J. Polym. Sci., Part B: Polym. Phys.* **1989**, *27*, 1029.
(30) Albrecht, T.; Strobl, G. *Macromolecules* **1996**, *29*, 783.
(31) Akpalu, Y. A.; Amis, E. J. *J. Chem. Phys.* **2000**, *113*, 392.
(32) Jackson, J. F.; Mandelkern, L. *Macromolecules* **1968**, *1*, 546.
(33) Weaver, T. J.; Harrison, I. R. *Polymer* **1981**, *22*, 1590.
(34) Runt, J.; Harrison, I. R.; Varnell, W. D.; Wang, J. I. *J. Macromol. Sci., Phys.* **1983**, *B22*, 197.
(35) Passaglia, E.; Khoury, F. *Polymer* **1984**, *25*, 631.
(36) Blundell, D. J.; Keller, A.; Kovacs, A. J. *J. Polym. Sci., Polym. Lett.* **1966,** *4*, 481.
(37) Additional information on the "X-ray" software are available on request to M. Dosière (e-mail: dosiere@umh.ac.be).
(38) Koch, M. H. J.; Bordas, J. *Nucl. Instrum. Methods* **1983**, *A208*, 461.
(39) Boulin, C. F.; Kempf, R.; Gabriel, A.; Koch, M. H. J. *Nucl. Instrum. Methods* **1988**, *A269*, 312.
(40) Strobl, G. R.; Schneider, M. J. *J. Polym. Sci., Polym. Phys. Ed.* **1980**, *18*, 1343.
(41) Mizushima, S.; Shimanouchi, T. *J. Am. Chem. Soc.* **1949**, *71*, 1320.
(42) Courtesy of late A. Keller.
(43) Ungar, G.; Stejny, J.; Keller, A.; Bidd, I.; Whiting, M. C. *Science* **1985**, *229*, 386.
(44) Strobl, G. R.; Eckel, R. *J. Polym. Sci., Polym. Phys. Ed.* **1976**, *14*, 913.
(45) Schaufele, R. F.; Shimanouchi, T. *J. Chem. Phys.* **1967**, *47*, 3605.
(46) Snyder, R. G.; Krause, S. J.; Scherer, J. R. *J. Polym. Sci., Polym. Phys. Ed.* **1978**, *16*, 1593.
(47) Snyder, R. G.; Scherer, J. R. *J. Polym. Sci., Polym. Phys. Ed.* **1980**, *18*, 421.
(48) Fraser, G. V. *Indian J. Pure Appl. Phys.* **1978**, *16*, 344.
(49) Keller, A.; Sawada, S. *Makromol. Chem.* **1964**, *74*, 190.
(50) Labaig, J.-J. Ph.D. Thesis, Université Louis Pasteur de Strasbourg, 1978.
(51) Khoury, F.; Boltz, L. H. *Proc. 38th Ann. Proc. Electron Microsc. Soc. Am.* **1980**, 242.
(52) Khoury, F.; Fanconi, B.; Barnes, J. D.; Bolz, L. H. *J. Chem. Phys.* **1973**, *59*, 5849.
(53) Jackson, J. F.; Mandelkern, L. *Macromolecules* **1968**, *1*, 546.
(54) Huseby, T. W.; Bair, H. E. *J. Appl. Phys.* **1968**, *39*, 4969.
(55) Ergoz, E.; Mandelkern, L. *J. Polym. Sci., Polym. Lett. Ed.* **1973**, *11*, 73.
(56) Sanchez, I. C.; DiMarzio, E. A. *Macromolecules* **1971**, *4*, 677.
(57) Pennings, A. J. In *Characterization of Macromolecular Structure*; Publication No. 1573; National Academy of Sciences: Washington, DC, 1968; p 214.
(58) Wunderlich, B. *Macromolecular Physics*; Academic Press: New York, 1980; Vols. 1 and 3.
(59) Hobbs, J.; Barham, P.; Keller, A. *Proc. PMSE* **1999**, *81*, 223.
(60) Sadler, D. M. *J. Polym. Sci., Part A-2* **1971**, *9*, 779.
(61) Dosière, M.; Colet, M.-Ch.; Point, J.-J. In *Morphology of Polymers*; Sedlacek, B., Ed.; 1986; p 171.
(62) Sanchez, I. C.; DiMarzio, E. A. *J. Res. Natl. Bur. Stand., Sect. A* **1972**, *76A*, 213.
(63) Point, J.-J.; Colet, M.-Ch.; Dosière, M. *J. Polym. Sci., Polym. Phys. Ed.* **1986**, *24*, 357.
(64) Leung, W. M.; Manley, R. St. J.; Panaras, A. R. *Macromolecules* **1985**, *18*, 760.
(65) Dosière, M.; Colet, M.-C.; Point, J.-J. *J. Polym. Sci., Polym. Phys. Ed.* **1986**, *24*, 345.

MA011974U